MUHAMMAD HAMMAD SAEED[1*], WANG FANGZONG[1], MD FAISAL BIN ASHAB[1], RAKIBUL ISLAM[1]

J. Electrical Systems 20-1 (2024): 1-16

Regular paper

Autonomous DC Microgrid's Coordinated Control Consisting of Photovoltaic Generation and Energy Storage System

This paper proposes a hierarchical coordinated control technique for a photovoltaic and energy storage units-based autonomous DC microgrid. The primary layer controls photovoltaic and energy storage units. As a result, the converters in every unit can change the bus voltage autonomously. Multiple energy storage groups are coordinated through adaptive droop control, which automatically distributes load power across various energy storage units based on maximum power and state of charge. This scheme stabilizes the bus voltage. When the needed charging power for the energy storage system exceeds the maximum permissible power, the photovoltaic system transitions from maximum power tracking (MPPT) control to droop mode to ensure the bus voltage stability. So, multiple photovoltaic units can automatically distribute load power based on their maximum powers. Simultaneously, to raise the bus voltage to the rated value, the voltage feedforward compensation control is also exploited to modify the droop controller s reference voltage dynamically. The secondary layer coordinates the operating modes of various converters in accordance with the bus voltage to guarantee that all converters manage the DC voltage in compliance with the voltage droop characteristics to maintain the system s active power balance. Eventually, a simulation model is developed in Matlab/ Simulink to evaluate the effectiveness of the proposed hierarchical control strategy in three different operating conditions. The simulation results demonstrate that hierarchical coordinated control can ensure the autonomous DC microgrid s stable operation.

Keywords:DC Microgrid (DCMG); Droop Control, Energy Storage System (ESS); Energy Storage Units (ESUs); Hierarchical Control; MPPT Control; State of Charge (SOC); Voltage Feedforward Control; Stability.

1. Introduction

Recent years have seen an increase in the penetration rate of distributed new energy generation, such as wind and solar energy [1–4], and nations worldwide are paying more attention to new energy development [5]. Microgrids (MGs) are a new type of emerging power grid that incorporates controllable loads, energy storage systems, distributed power sources, and other elements [6, 7]. MGs can function in two operational modes, namely autonomous and grid-tied [5], and could be AC or DC depending upon the generation sources, flexible power supply modes, loads, and area of service [8]. Most MG research focuses on the AC MG because the conventional power system is an AC system. However, many modern energy sources, including energy storage devices and distributed power sources like fuel cells, photovoltaic, and wind, have DC output forms. These sources' DCMGs can successfully connect the source to loads. They offer high-quality power for DC loads and can lower AC-DC conversion losses and costs [9, 10]. In addition, there are no problems with phase synchronization, harmonics, and reactive power loss in DCMGs.

* Corresponding author: M.H. Saeed, College of Electrical Engineering & New Energy, China Three Gorges University, 443000, P.R. China, E-mail: muhammad005@ctgu.edu.cn
[1]College of Electrical Engineering & New Energy, China Three Gorges University, 443000, P.R. China

Therefore, the DCMG power supply mode has gradually become a vital research hotspot in recent years [11]. Conversely, the intermittent and erratic behavior of renewable energy resources (RERs) makes the DCMG system challenging and unique. Stand-alone/autonomous DCMGs depend on energy storage systems to sustain demand levels and enhance power quality because RERs are sporadic [12, 13].

The bus voltage is an essential indicator of the power system's stability and balance [14-17]. To maintain voltage stability, the authors of Ref. [18] developed a hierarchical coordinated control technique for wind power DCMG. The control strategy for each power electronic converter is provided at various control levels. This method effectively controls the bus voltage's stability by automatically adjusting the voltage in small steps based on the voltage variation range. The authors developed a coordinated secondary control strategy for an autonomous hybrid three-port AC/DC/DS microgrid with distributed power management in Ref. [19]. The proposed control technique can regulate AC and DC voltages at nominal values while maintaining local power-sharing, global power-sharing, storage power-sharing, and distributed power management using a low bandwidth communication system with limited and speed-insensitive information flow. To swiftly track the expected voltage and ensure the system's robustness and stability, Ref. [20] adopted a sliding mode control method based on linearized feedback to control the DC bus voltage. The simulation verified the validity and accuracy of the suggested control mechanism in the DC/DC conversion of the bidirectional DCMG system. For controlling the operating point stability of large-scale power converters, the control approach has a straightforward algorithm and a reliable reference value. DCMGs typically use energy storage units (ESU) to stabilize the power fluctuations of distributed power sources and preserve source-load power balance. The authors of Ref. [21] proposed a novel energy management control strategy for a smart DCMG employing a combination of high-order sliding mode (HSMC) and fuzzy logic controller (FLC) techniques. The proposed intelligent control optimizes energy capture from hybrid renewable energy sources (wind, tidal, and PV) while boosting DCMG power quality by regulating source-side converters (SSCs).

Huo et al. presented a communication-less power management strategy for multiple-DAB-based ESS to realize maintenance and extend the capacity of the ESS [22]. The control strategy ensured the high robustness of the dc-link voltage when the input voltages and load conditions vary, or an energy storage unit (ESU) is plugged-in or -out. Chowdhury et al. discussed a Battery Management system for a series string of Li-ion battery cells by developing a dynamic droop control theory consisting of one closed-loop structure [23]. The proposed architecture is adaptable to any power level by including the cell-converter structure. However, on the other hand, the power processing dc/dc converter for the traditional system still requires a new design.

Azizi et al. proposed autonomous energy management and power-sharing technique for DCMGs. The proposed method does not necessitate supervisory control or communication infrastructure [24]. The suggested approach can successfully manage the PV unit and interlinking converter operations. However, this control strategy is limited to non-MPPT-based units. Shi et al. presented a novel DG control strategy for MG islanding using phasor measurements at the point of common coupling [25]. The proposed controller adapts DG

outputs to compensate for a system power imbalance during the transition. However, The approach is only applicable to the three-phase balanced MG. Kulkarni & Gaonkar proposed a robust control strategy with a virtual impedance control-based droop control for power-sharing with f/V restoration [26]. However, the droop controller state-space small-signal model was investigated for large-scale MG.

Based on the above literature review, this article presents a hierarchical coordinated control strategy for an autonomous photovoltaic-storage-DC microgrid. The maximum power tracking control (MPPT) and droop control are designed for the PV system, respectively, to maintain the bus voltage stability under the control of the first layer. The photovoltaic system switches from the maximum power control mode to the droop control mode when the charging power of the energy storage system (ESS) surpasses its maximum permitted power. This automatically distributes the load power of various PV- units and maintains voltage stability. In addition, the voltage feedforward compensation control is used to adjust the droop control mode dynamically. The voltage reference of the controller increases the bus voltage to the rated value. In order to keep the bus voltage stable for ESS, adaptive droop control coordinates various energy storage units (ESUs). It also automatically distributes the load power among various ESUs based on the maximum power and SOC. The secondary control layer coordinates the operational modes of different converters according to the bus voltage to ensure that in different working modes, all converters control the DC voltage according to the voltage droop characteristics to maintain the balance of active power in the system.

This article has been structured as follows: Section 2 represents the model of DCMG. Section 3 describes the three different operational modes of the autonomous DCMG. Section 4 elaborates on the control strategy with sub-section 4.1 describing the Primary Control and sub-section 4.2 the Secondary Control. Section 5 discusses the simulation results for all three working modes, and finally, Section 6 concludes this work.

2. Model of DCMG

Figure 1 shows the model of the DCMG, consisting of photovoltaic systems, ESS, and AC and DC loads [27].

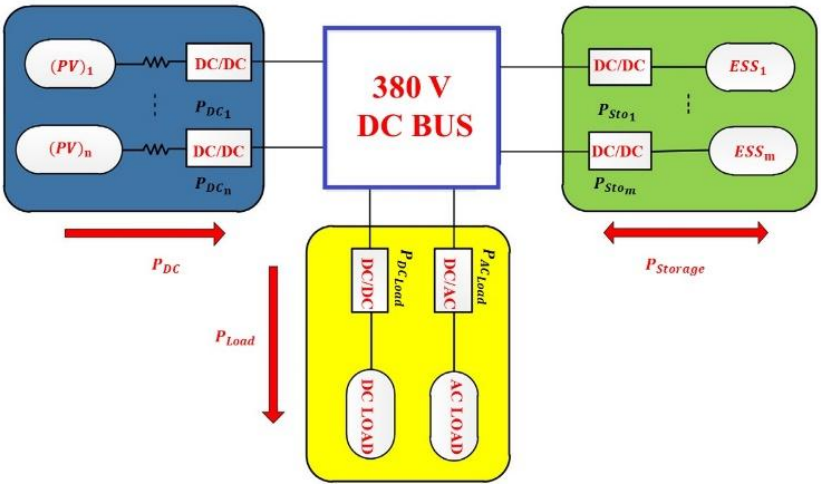

Fig. 1 Model of DC Microgrid

InFig. 1, n and m are the numbers of photovoltaic and ESUs, respectively. And,

$P_{DC_n}$is the power generated by the n[th] photovoltaic unit and $P_{DC_n} = \sum_{i=1}^{n} \mathrm{P}_{\mathrm{DC}_i}$

$P_{DC_{Load}}$ and $P_{AC_{Load}}$are the DC and AC load power respectively,

where, $P_{load} = P_{DC_{Load}} + P_{AC_{Load}}$

V_{DC} is the DC bus- voltage. $P_{Sto_m}$is the power of the m[th] ESU, $P_{Sto} = \sum_{i=1}^{m} \mathrm{P}_{\mathrm{Sto}_i}$.

The output current of the photovoltaic system is: [27- 30].

$$I = I_{ph} - I_d \left[e^{\frac{q(U+IR_S)}{AkT}} - 1 \right] - \frac{U+IR}{R_{sh}} \quad (1)$$

Here,

$R_{sh}$and R_s are equivalent parallel-series impedances respectively, I_{ph} and I_d are the photocurrent and the diode's reverse leakage current, respectively. U and I are the terminal voltage and output current of the photovoltaic system, respectively. T is the photovoltaic temperature, q is the electronic charge, and k is the Boltz-Mann constant. The output voltage of the ESU is: [30- 32].

$$V_b = V_o + R_b . i_b - K \frac{Q}{Q + \int i_b dt} + C . e^{B \int i_b dt} \quad (2)$$

$$SOC = 100 \left(1 + \frac{\int i_b dt}{Q} \right) \quad (3)$$

In these formulas: R_b is the internal resistance of the battery, V_b is the terminal voltage of the battery, V_o is the battery open-circuit voltage, i_b is the battery charging current, K is the battery polarization voltage, Q is the battery capacity, B and C are fitting coefficients.

3. DCMG Operational Modes

Three different operating modes are taken into consideration in order to validate the impact of the control approach. The DCMG functions in the following three modes:

1) Mode I: The ESS stabilizes the bus voltage

In this mode, the PV- system utilizes MPPT control, and the ESS employs adaptive droop control to stabilize the voltage through the bidirectional converter and smoothen the fluctuations in PV-generated power. The ESS's current output is:

$$P_{Sto} = P_{Load} - P_{DC} \quad (4)$$

2) Mode II: Some of the ESUs or PV- units are out of operation

This operating mode focuses on the scenario when particular PV- units and ESUs are down for maintenance or out of connection for some reason, and the remaining ESUs regulate the bus voltage. The PV system still operates under MPPT control. The regular operation of the ESU automatically adjusts the output power to compensate for the malfunctioning ESU's power to maintain the stability of the bus voltage. The ESS can automatically adjust the output power according to the bus voltage to ensure the normal power supply to the load when the PV system is partially or entirely out of operation. During this mode, the ESS's current output is:

$$P_{Sto} = \sum_{i=1}^{u} P_{Sto_i} = P_{Load} - P_{DC} \quad (5)$$

Here, u is the number of ESUs during normal working conditions, and $u \leq n$.

In particular, when ESS's discharge power required in the DCMG exceeds its maximum allowable output power, the insufficient active power will cause the bus voltage to drop. Meanwhile, to ensure the normal power supply to the critical loads, it is necessary to cut off the secondary loads according to the load priority to ensure the active power balance of the system.

3) Mode III: The PV system stabilizes the bus voltage

When the ESS's charge power surpasses the maximum allowable power, the excess active power will cause the bus voltage to rise, and the DCMG goes into operating mode III. At this point, it is necessary to control the PV system to reduce the power generation to keep the bus-voltage stable. The output power of the photovoltaic system is :

$$P_{DC} = P_{Load} \tag{6}$$

In particular, the ESS could balance the supply and demand of active power in the MG by discharging when the PV system's power cannot meet the normal supply due to irradiance or load power variations. The normally running PV units immediately adjust the power generation and take over the output power of the malfunctioning units. If v $(and\ v \leq m)$ is the number of PV units during normal working conditions, the system's power at this moment will be:

$$P_{DC} = \sum_{i=1}^{v} P_{DC_i} = P_{Load} \tag{7}$$

4. Control Approach

This paper proposes a hierarchical coordinated control strategy to control the bus voltage stability in an autonomously functioning DCMG.

4.1. Primary Control

The bus voltage directly affects the stable operation of the DCMG system, so it is necessary to control the bus voltage to the allowable range and balance the supply and demand of the source load power in the MG. The photovoltaic and energy storage systems operate independently under the primary control layer.

4.1.1. Control of PV System

The ESS sustains the bus voltage when the DCMG is in modes I and II, and the PV system operates under MPPT control. The PV system switches to droop control in mode III. The control scheme for the PV system operating in mode III is shown in Figure 2. It adjusts the generated power by the load power to maintain the bus voltage. Consequently, it applies voltage feedforward control and automatically adjusts the load power distribution among the PV units based on their maximum power. The second layer control provides the switching signal M after the compensating control has raised the bus voltage to its rated value.

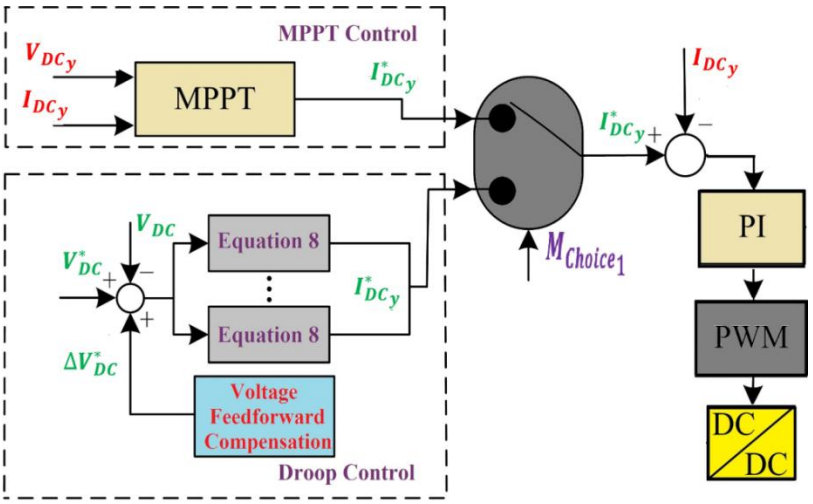

Fig. 2 Control of PV System

Here, I_{DC_y} and V_{DC_y} are the output current and terminal voltage of the y[th] PV unit, respectively. $I^*_{DC_y}$ and V^*_{DC} are the reference values of current and voltage, respectively.

The droop characteristics of photovoltaic cells are [15]:

$$V_{DC_y} - I_{DC_y} Z_{DC_y} - V^*_{DC} = V_{DC} - V^*_{DC} = d_y P_{DC_y} \quad (8)$$

$$d_y = \frac{V^{min}_{DC} - V^{max}_{DC}}{P^{max}_{DC_y}} \quad (9)$$

In the above formulas, Z_{DC_y} is the output impedance of the y[th] photovoltaiccell, V^{max}_{DC} *and* V^{min}_{DC} are the maximum and minimum values of the output voltages of the PV system, and $P^{max}_{DC\ y}$ is the maximum power of the y[th] PV unit. The power of each PV unit is:

$$\frac{P_{DC_1}}{P^{max}_{DC_1}} = \frac{P_{DC_2}}{P^{max}_{DC_2}} \ldots\ldots = \frac{P_{DC_y}}{P^{max}_{DC_y}} = \frac{V_{DC} - V^*_{DC}}{V^{min}_{DC} - V^{max}_{DC}} \quad (10)$$

Equation (10) shows that each PV unit can autonomously change the power generated following its maximum power, which is advantageous to the voltage stability of the critical load in mode III. In order to reduce voltage fluctuations, feed forward compensation control is also used with the PV droop control (as illustrated in Figure 3). The disparity between the reference and bus voltages is detected. To achieve the dynamic compensation of the reference voltage to lessen bus voltage fluctuation, the compensation output from the PI controller is superimposed on the voltage reference value of the photovoltaic droop controller.

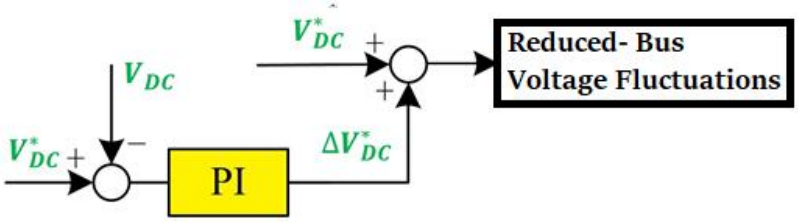

Fig. 3 Voltage Feedforward Control

4.1.2. Control of ESS

The ESS plays a paramount role to stabilize the bus voltage and minimizing the fluctuations by the intermittent energy resources. Following their maximum power and SOC, the adaptive droop control modifies the load power distribution among the ESS. Let us define:

$$\zeta = (\mathrm{V_{DC}})' \tag{11}$$

Here: ζ being constant, $\mathrm{V_{DC}}$ is the bus voltage. It can be formalized by Eq. (12) [15]:

$$(\mathrm{V_{DC}})' = \begin{cases} \frac{V_{DC}-V^*_{DC}}{V^{max}_{DC}-V^*_{DC}}, if\ V_{DC} > V^*_{DC} \\ \frac{V^*_{DC}-V_{DC}}{V^{min}_{DC}-V^*_{DC}}, if\ V_{DC} < V^*_{DC} \end{cases} \tag{12}$$

Giving, $-1 < (\mathrm{V_{DC}})' < 1$

The ESS discharges when $0 < (\mathrm{V_{DC}})' < 1$, and charges when $-1 < (\mathrm{V_{DC}})' < 0$. The output power of each ESS is:

$$\zeta = \mathrm{b_z} P_{Sto_z} \tag{13}$$

Here, P_{Sto_z} is the output power of the z[th] ESU, positive means discharge, negative means charging, $\mathrm{b_z}$ is the droop coefficient of the z[th] ESU droop controller.

$$b_z = \begin{cases} \frac{\left(\frac{SOC_z}{SOC^*_z}\right)^{\lambda}}{P_{Sto_z}{}^{max}}, if\ P_{Sto_z} < 0 \\ \frac{\left(\frac{SOC^*_z}{SOC_z}\right)^{\lambda}}{P_{Sto_z}{}^{max}}, if\ P_{Sto_z} > 0 \end{cases} \tag{14}$$

Where, $P_{Sto_z}{}^{max}$ is the maximum power of the z[th] ESU, SOC_z is the instantaneous value and SOC^*_z is the reference value of the state of charge of the z[th] ESU, $\lambda = 1$ and $SOC^*_z = 0.5$. Therefore, each ESU can adjust the load power distribution through adaptive droop control according to its SOC.

$$\frac{P_{Sto_1}}{P_{Sto_1}{}^{max}} = \frac{P_{Sto_2}}{P_{Sto_2}{}^{max}} = \frac{P_{Sto_3}}{P_{Sto_3}{}^{max}} = \ldots\ldots = \frac{P_{Sto_m}}{P_{Sto_m}{}^{max}} = \begin{cases} \left(\frac{SOC_z}{SOC^*_z}\right)^{\lambda}.\zeta & ;\text{Charge} \\ \left(\frac{SOC^*_z}{SOC_z}\right)^{\lambda}.\zeta & ;\text{Discharge} \end{cases} \tag{15}$$

The automatic load power distribution among the ESUs facilitates promptly balancing the SOC of various ESUs. It prevents the ESS from being overcharged or over-discharged, increasing the ESS's protection. The battery energy management system is responsible for keeping the battery's charging and discharging power and capacity within a specific range to prolong battery life [25]. The SOC rating for this work is between 10% and 90%. The charging current is nil when the

SOC hits 90%. When the SOC drops to 10%, the ESS keeps discharging to guarantee the critical load's voltage stability. Nevertheless, in order to protect the battery, load shedding should be done in a priority-based manner. The ESS's control approach is depicted in Fig. 4.

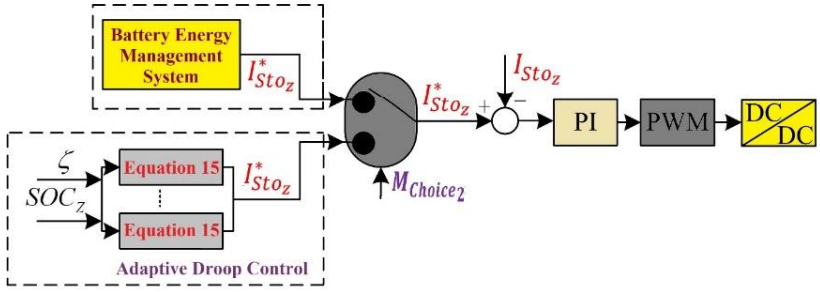

Fig. 4 Control of ESS

Where, $I_{Sto_z}$is the current of the z[th] ESU, and $I^*_{Sto_z}$is its reference value. The mode switching signal M_{Choice_2} is given by the second layer control.

4.1.3. Load Control

The converter connects the AC and DC loads to the DC bus. Fig. 5 shows the load power control. Loads can be prioritized according to their importance to ensure a stable power supply for critical loads.

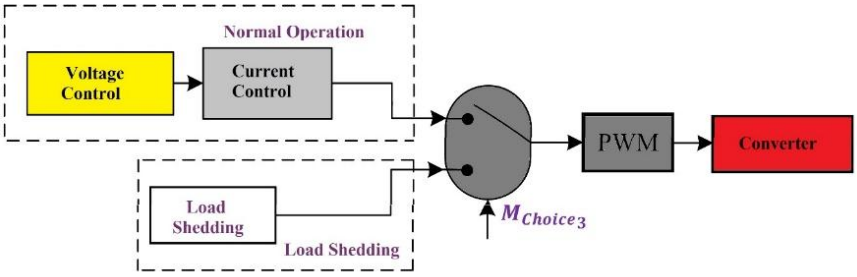

Fig. 5 Control of Load Converter

4.2. Secondary Control

Figures 6 and 7 depict the DCMG's secondary control and working logic diagram, respectively. It exploits the bus voltage signal to regulate the power flow in the DCMG and the PV system's switching between operating modes to reduce power loss significantly. The vital purpose of the secondary control is to use the bus voltage to regulate the output power of the ESS in modes I and II, as well as the mode switching of the PV system. Moreover, the ESS stabilizes the bus voltage by adopting adaptive droop control and automatically adjusts the load power distribution among the ESUs according to their respective maximum power and SOC, which improves the safety of the ESS. When operating in mode III, the PV system switches from MPPT to droop control to control the bus voltage stability, and each PV unit automatically adjusts the load power distribution according to the maximum output capacity. Furthermore, the voltage feedforward compensation control adjusts the voltage reference value of the PV droop controller

to increase the bus voltage to the rated value. Consequently, the bus voltage fluctuation reduces. Let us define:

$$\left|\left(V_{DC} - \varepsilon_{V_{DC}}\right)^{'}\right| > \left|\left(V_{DC}\right)^{'}\right|_{s} \tag{16}$$

Here, $\left|\left(V_{DC}\right)^{'}\right|_{s} = 0.2$ and $\varepsilon_{V_{DC}}$ is the voltage fluctuation value. The ESS does not execute power exchange to reduce power loss when the bus voltage fluctuates within this range. The ESS charges or discharges to stabilize the bus voltage when the bus voltage fluctuations go beyond this range. Additionally, the layer control sends the mode switching signal $M_{choice_1} - M_{choice_3}$ according to equation (16) and the control logic.

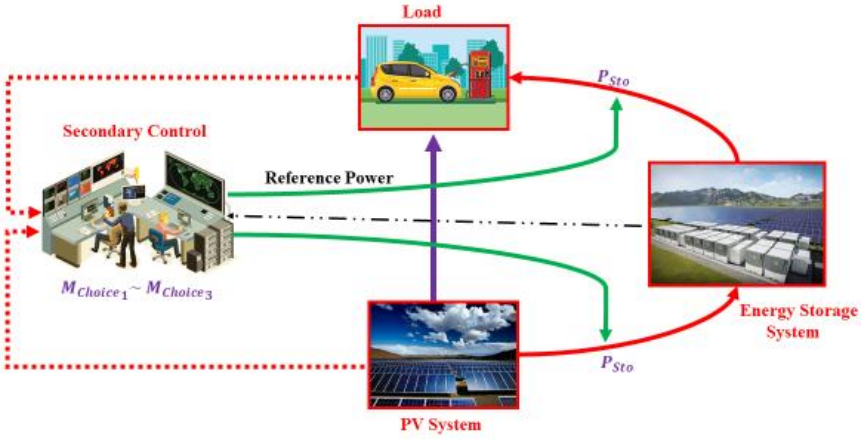

Fig. 6 Secondary Control of Autonomous DCMG

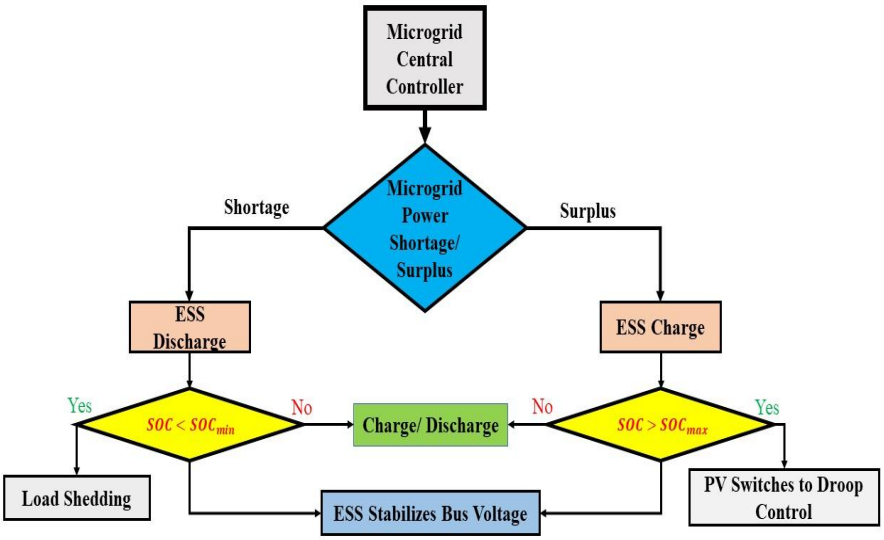

Fig. 7 Working Logic of Autonomous DCMG

5. Simulation Results and Discussion

A simulation model was built in Matlab/Simulink for a DC Bus of 380 volts to demonstrate the efficiency of the suggested hierarchical control strategy. Three ESUs with 4.5 kWh each and two sets of PV generation units with a maximum output of 2 kW and 4 kW compose the model. The highest output power is ± 3 kW, ± 2 kW, and ± 2 kW, respectively, with SOCs of 80%, 60%, and 40%. The safe charging capacity is not higher than 90%, and the safe discharge capacity is no less than 10%. Three different working modes are taken into account in the simulation, and variable loads are connected to evaluate the system's response to disturbances such as load fluctuations.

1) Mode I

The PV system uses MPPT control in this mode, and the ESS is responsible for maintaining bus voltage stability. The configuration of multiple groups of small-capacity ESUs to lower the converter's current increases the ESS's protection. The simulation examines how disturbances in load power and fluctuation generated by PV systems affect bus voltage. Figure 8 shows the simulated waveforms when the ESS stabilizes the bus voltage. It can be seen from Figure 8 that at 0~1.0 s, the PV system adopts MPPT control. The load power at this moment is 3.6 kW, the PV system's power is 4.5 kW, and the ESS needs to provide 1.8 kW of load power to ensure the regular operation of the MG and voltage stability. The load power provided by the ESS stabilizes bus voltage.

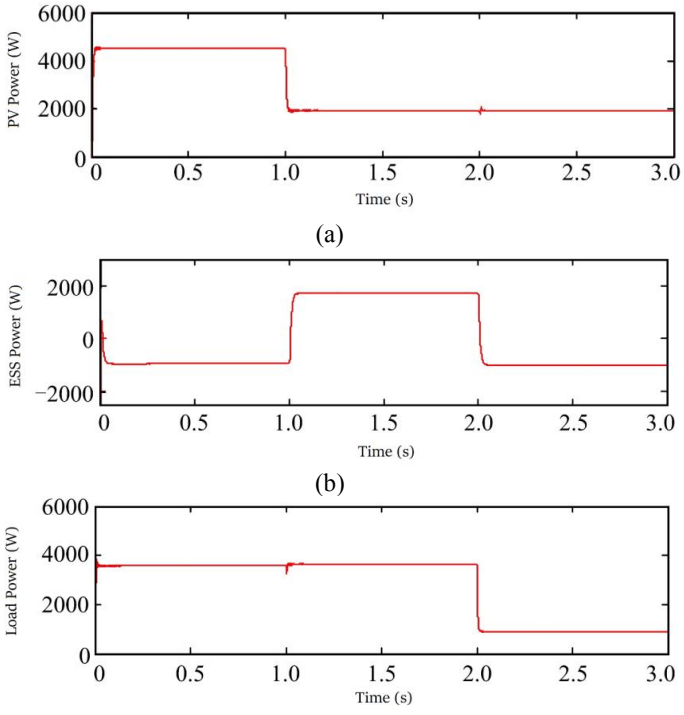

Fig. 8 Operation Performance of DCMG working in Mode I (a) PV System Output Power (b) Power by ESS (c) Load Power

The charging power of the ESS at this time is around 0.9 kW, and the bus voltage is controlled at 379 V in this mode, as can be shown by comparing Figs. 8(b) and 9. Due to irradiance fluctuations, the PV power reduces by about 2.0 kW in 1.0 s. The ESS instantly adjusts the output power to approximately 1.6 kW to ensure voltage stability and the regular operation of the system. At 2.0 s, the load power drops to about 1.0 kW while the PV power remains at 2.0 kW. The ESS quickly transitions from the discharge state to the charging state. For the system's active power balance and bus voltage stability, it supplies about 1.0 kW of power. Figure 8 shows that the ESS can seamlessly switch between the charging and discharging modes when the source load power varies. As a result, the system's supply and demand for active power are efficiently balanced. Figure 9 shows that the bus voltage fluctuation is minimal under various disturbances and that the response time is short.

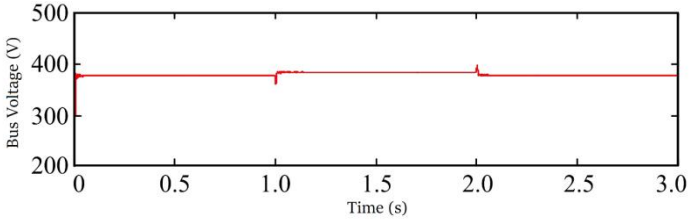

Fig. 9 Bus voltage of DCMG

The load power distribution among the ESUs is shown in Figure 10. It gives a comparison of the proposed adaptive droop control and the conventional droop control. It is obvious that the adaptive droop control can automatically adjust the load power distribution according to the SOC and maximum power of various ESUs when compared to the conventional droop control. As a result, it can quickly balance the SOC between several ESUs and prevent overcharging of the ESS. Additionally, the fluctuation is minimal, and the switching between the charging and discharging modes happens quickly.

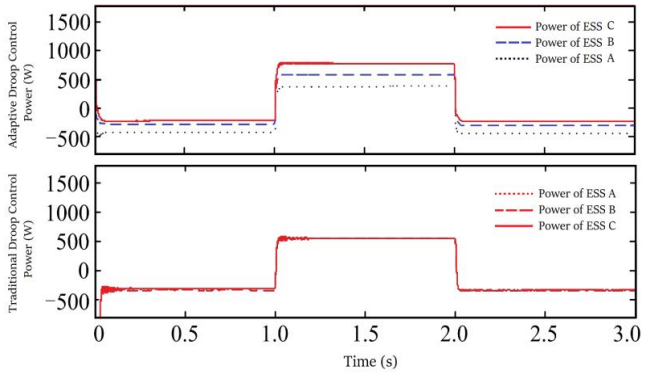

Fig. 10 Comparison ofPower Sharing among Energy Storage Units (With Proposed Adaptive Droop Control and with Traditional Droop Control)

2) Mode II

In this mode, the ESS stabilizes the bus voltage while the PV system continues to perform MPPT control. The simulation of Fig. 11 examines the bus voltage's stability in the presence of disturbances and Fig. 12 shows the Bus voltage during these conditions. The ESS stabilizes the bus voltage at 0~1.0 s, at which point the PV system adopts MPPT control. The load power is 2.6 kW, but the PV system's power is about 5.1 kW. The bus voltage is controlled at 382 V, and

the ESS's charging power at this point is 2.5 kW, as illustrated in Figure 12. A group of ESUs in the ESS is out of operation due to faults and at 1.0 s. The ESUs in normal operation swiftly adjust the output power to provide a normal power supply to the load to ensure voltage stability and normal system operation. The ESS's overall charging capacity is still 2.5 kW at this moment. The PV system's power output falls to zero at 2.0 seconds. The normal operation of the ESUs is then immediately transitioned from the charging to the discharging state to guarantee the load receives normal power. With quick switching and smaller bus voltage variations, they begin to supply the load with about 2.6 kW of power. It is evident from the above analysis that the bus voltage fluctuation is negligible, the response time is quick, and the load voltage fluctuation successfully reduces when the PV system and (or) ESUs are not functioning.

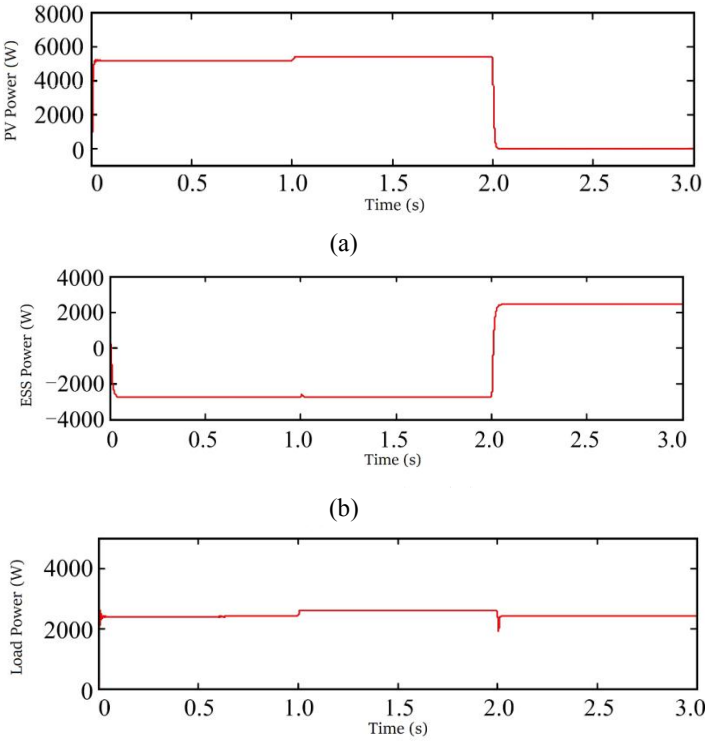

Fig. 11 Operation Performance of DCMG working in Mode II (a) PV System Output Power (b) ESS Power (c) Load Power

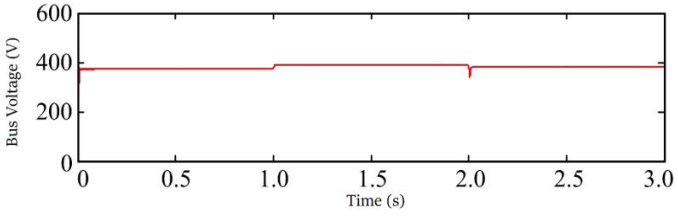

Fig. 12 Bus voltage of DCMG

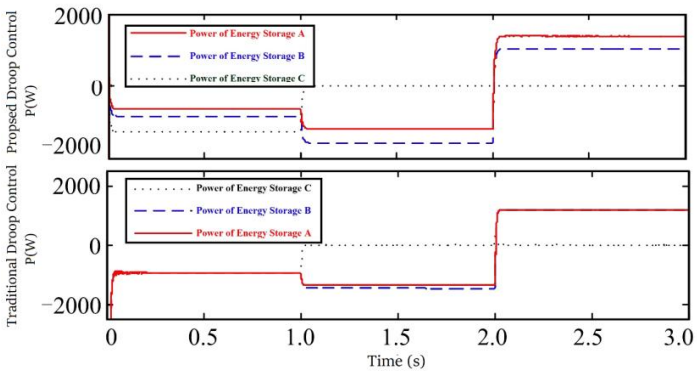

Fig. 13 Power sharing among storage units (With Proposed Droop Control and with Traditional Droop Control)

Figure 13 shows the load power distribution among the ESUs in mode II. The ESS can automatically adjust the load power distribution among the ESUs according to the maximum power and SOC by operating under the proposed adaptive droop control. When some ESUs or PV units fail, the ESUs in normal operation can promptly compensate for the output power to meet the normal power supply to the load, reducing the bus voltage fluctuation and sustaining the voltage stability. In addition, the use of multiple groups of small-capacity energy storage can reduce the current of the converter and improve the protection of the ESS.

3) Mode III

This mode deals with the scenario when the battery reaches the capacity limit due to the PV system producing more energy than the DCMG's load requirement. The PV system switches from MPPT to droop control to ensure the voltage stability of the critical loads. As a result, the output power changes automatically to meet the load demands. The simulations in Fig. 14 analyze the influence of disturbances such as the ESS and PV system failures and load fluctuations on the voltage stability. When the PV system switches to MPPT control at time 0~1.0 s, the energy storage stabilizes the bus voltage. The PV system power is approximately 4.7 kW, the ESS charging power is 0.6kW, and the load power is 4.1 kW. The switching process has a quick response time and negligible variation, as demonstrated in Fig. 14. When PV unit 1 stops working at 2.0 s, PV unit 2 swiftly adjusts the generated power to guarantee uninterrupted power to critical loads. Following that, the PV unit 2 automatically adjusts the power output based on the load's power requirements and performs necessary load shedding to maintain the regular power supply to critical loads.

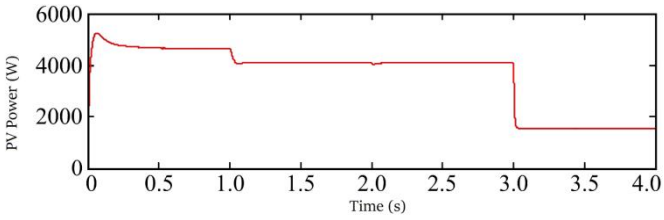

(a)

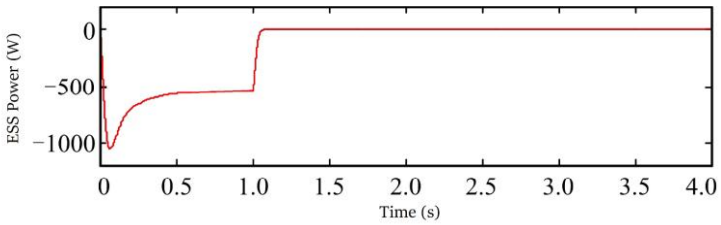

(b)

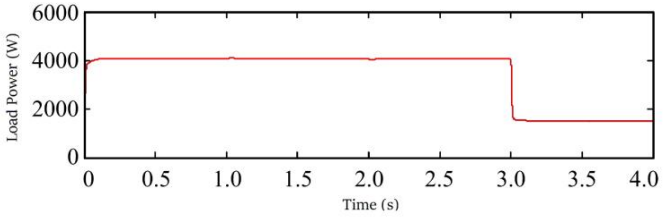

(c)

Fig. 14 Operation Performance of DCMG working in Mode III (a) PV System Output Power (b) ESS Power (c) Load Power

Figure 15 depicts the load power distribution in the PV units. After the ESS is disconnected, the PV unit adopts droop control at time 1.0–2.0s. The load power distribution among the PV units differs due to the difference in maximum output power. Each PV unit automatically adjusts the load power distribution based on its maximum power to ensure the system's smooth operation. In particular, if the PV unit 2 cannot meet the load power supply, the load shedding operation needs to be performed according to the load priority to sustain a stable voltage to the critical loads.

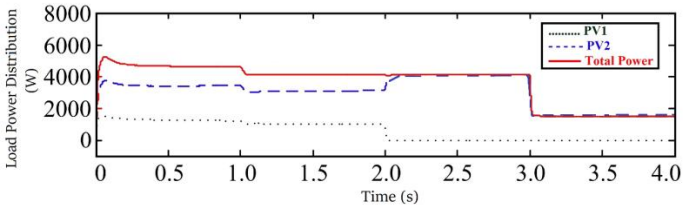

Fig. 15 Power Sharing among PV units

Fig. 16 elaborates on the bus voltage without and with proposed feedforward compensation control. The comparison of Figures 16(a) and (b) shows that the proposed voltage feedforward compensation control effectively reduces the fluctuations in the bus voltage in the PV droop control mode. The above analysis shows that the switching between MPPT and droop control of the PV system is beneficial to ensure the voltage stability of critical loads.

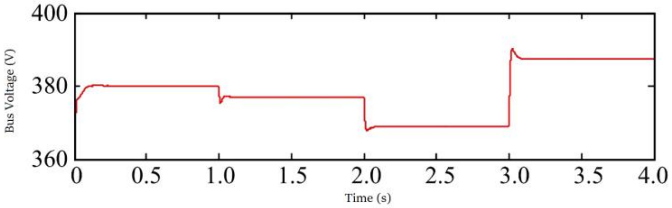

(a)

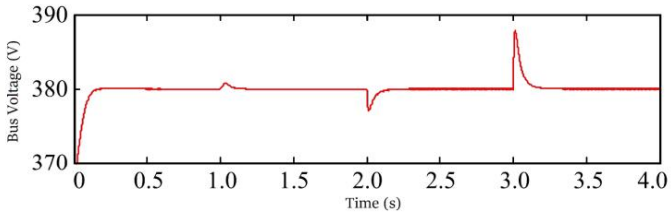

(b)

Fig. 16 Bus voltage of DCMG (a) Without Voltage Feedforward Control (b) With Voltage Feedforward Control

6. Conclusion

This study provides a hierarchical coordinated control strategy for an autonomous DC microgrid based on an ESS and a PV system. The primary layer controls the PV units and ESS to operate autonomously. Each unit's converters can independently adjust the bus voltage. When the required charging power of the ESS in the DCMG exceeds its maximum allowable power, the PV system switches to droop control to stabilize the bus voltage. Concurrently, the voltage feedforward control is adopted to reduce the bus voltage fluctuation. By considering the maximum power and SOC of each ESU, adaptive droop control is executed to coordinate the automatic distribution of load power among the units. The secondary control layer coordinates the working modes of various converters according to the bus voltage to increase system effectiveness and voltage stability. This ensures that the converters droop according to the voltage in different working modes. The Matlab/Simulink platform is used to build a simulation model. According to the simulation results, the proposed control method successfully reduces bus voltage fluctuations while preserving the autonomous DMG's reliable operation.

Conflict of Interest

The author declares that there is no conflict of interest by any means.

References

[1] M. J. Rahman, T. Tafticht, and M. L. Doumbia, “Power Stability and Frequency Control Techniques of DG for a High Penetration Wind-Based Energy Storage System Using Integral- Derivative Controller,” IEEE Canadian Journal of Electrical and Computer Engineering, pp. 1-10, 2021. DOI: 10.1109/ICJECE.2021.3103524.

[2] O. H. Sebastian, M. Juan, F. Fredes, and E. Sauma, “Impact of increasing transmission capacity for a massive integration of renewable energy on the energy and environmental value of distributed generation,” Renewable Energy, vol. 183, pp. 524-534, 2022. DOI: 10.1016/j.renene.2021.11.025.

[3] Z. A. Khan, T. Hussain, and S. W. Baik, “Boosting energy harvesting via deep learning-based renewable power generation prediction,” Journal of King Saud University – Science, vol. 34, no. 3, article no. 101815, 2022. DOI: 10.1016/j.jksus.2021.101815.

[4] M. H. Saeed, W. Fangzong, and B. A. Kalwar, “Control of Bidirectional DC-DC Converter for Micro-Energy Grid’s DC Feeders' Power Flow Application,” International Journal of Renewable Energy Development, vol. 11, no. 2, pp. 533-546, 2022. DOI: 10.14710/ijred.2022.41952.

[5] M. H. Saeed, W. Fangzong, B. A. Kalwar, and S. Iqbal, “A Review on Microgrids’ Challenges & Perspectives,” IEEE Access, vol. 9, pp. 166502-166517, 2021. DOI: 10.1109/ACCESS.2021.3135083.

[6] [6] B. F. Bastos, C. R. Aguiar, A. Balogh, Z. Sütő, and R. Q. Machado, “Power-sharing for dc microgrid with composite storage devices and voltage restoration without communication,” International Journal of Electrical Power & Energy Systems, vol. 138, article no. 107928, 2022. DOI: 10.1016/j.ijepes.2021.107928.

[7] M. H. Saeed, W. Fangzong, S. Salem, Y. A. Khan, B. A. Kalwar , A. Fars, “Two-stage intelligent planning with improved artificial bee colony algorithm for a microgrid by considering the uncertainty of renewable sources,” Energy Reports, vol. 7, pp. 8912-8928, 2021. DOI: 10.1016/j.egyr.2021.10.123.

[8] S. Monesha, S. G Kumar, and M. Rivera, “Methodologies of Energy Management and Control in Microgrid,” IEEE Latin America Transactions, vol. 16, no. 9, pp. 2345-2353, 2018. DOI: 10.1109/TLA.2018.8789554.

[9] A. A. Bajwa, H. Mokhlis, S. Mekhilef, and M. Mubin, “Enhancing power system resilience leveraging microgrids: A review,” Journal of Renewable and Sustainable Energy, vol. 11, article no. 035503, 2019. DOI: 10.1063/1.5066264.

[10] P. Singh and J. S. Lather, “Power management and control of a grid-independent DC microgrid with hybrid energy storage system,” Sustainable Energy Technologies and Assessments, vol. 43, article no. 100924, 2021. DOI: 10.1016/j.seta.2020.100924.

[11] L. –L. Fan, V. Nasirian, H. Modares, F. L. Lewis, Y. –D. Song, and A. Davoudi, "Game-theoretic control of active loads in DC microgrids," IEEE Transactions on Energy Conversion, vol. 31, no. 3, pp. 882-895, 2016. DOI: 10.1109/TEC.2016.2543229.

[12] A. M. Gee, F. V. P. Robinson, and R. W. Dunn, "Analysis of battery lifetime extension in a small- scale wind-energy system using supercapacitors," IEEE Transaction on Energy Conversion, vol. 28, no. 1, pp. 24-33, 2013. DOI: 10.1109/TEC.2012.2228195.

[13] R. Kandari, P. Gupta, and A. Kumar, "Coordination Control and Energy Management of Standalone Hybrid AC/DC Microgrid," Journal of Engineering Research, vol. 9, pp. 58-69, 2021. DOI: 10.36909/jer.EMSME.13863.

[14] H. Bai, H. Zhang, and C. Li C, "Voltage regulation and current sharing for multi- bus DC microgrids," IFAC-PapersOnLine, vol. 53, no. 2, pp. 13018-13023, 2020. DOI: 10.1016/j.ifacol.2020.12.2166.

[15] S. K. Ghosh SK, T. K. Roy, M. A. H. Pramanik, and M. S Md Ali, "Energy management techniques to enhance DC-bus voltage transient stability and power balancing issues for islanded DC microgrids," In: Advances in Clean Energy Technologies. Academic Press, pp. 349-375, 2021. DOI: 10.1016/B978-0-12-821221-9.00009-8.

[16] Z. Shuai, J. Fang, F.Ning, Z. J. Shen, "Hierarchical structure and bus voltage control of DC microgrid," Renewable and Sustainable Energy Reviews, vol. 82, no. 3, article no. 3670-3682, 2018. DOI: 10.1016/j.rser.2017.10.096.

[17] S. Bagheri and H. M. CheshmehBeigi, "DC microgrid voltage stability through inertia enhancement using a bidirectional DC-DC Converter," 7th Iran Wind Energy Conference (IWEC2021), pp. 1-5, 2021. DOI: 10.1109/IWEC52400.2021.9467032.

[18] L. Zhang, Y. Wang, H. Li, and P. Sun, "Hierarchical coordinated control of DC microgrid with wind turbines," IECON 2012- 38th Annual Conference on IEEE Industrial Electronics Society, pp. 3547-3552, 2012. DOI: 10.1109/IECON.2012.6389329.

[19] C. Jin, J. Wang, and P. Wang, "Coordinated secondary control for autonomous hybrid three-port AC/DC/DS microgrid," CSEE Journal of Power and Energy Systems, vol. 4, no. 1, pp. 1-10, 2018. DOI: 10.17775/CSEEJPES.2016.01400.

[20] C. Liang, Y. Zhang, X, Ji, X. Meng, Y. An, and Q. Yao, "DC bus voltage sliding- mode control for a DC microgrid based on linearized feedback," 2019 Chinese Automation Congress (CAC), pp. 5380-5384, 2019. DOI: 10.1109/CAC48633.2019.8996266.

[21] M. S. Soliman, Y. Belkhier, N. Ullah, A. Achour, Y. M. Alharbi, A. A. Alahmadi, H. Abeida, and Y. S. H Khraisat, "Supervisory energy management of a hybrid battery/PV/tidal/wind sources integrated in DC-microgrid energy storage system," Energy Reports, vol. 7, pp. 7728-7740, 2021. DOI: 10.1016/j.egyr.2021.11.056.

[22] N. Hou, Y. W. Li, and L. Ding, "Communicationless power management strategy for the multiple DAB- based energy storage system in islanded DC microgrid," 2020 IEEE Energy Conversion Congress and Exposition (ECCE), pp. 4656-4661, 2022. DOI: 10.1109/ECCE44975.2020.9236420.

[23] S. M. Chowdhury, M. O. Badawy, Y. Sozer, and J. A. D. A. Garcia, "A Novel Battery Management System Using the Duality of the Adaptive Droop Control Theory," IEEE Transactions on Industry Applications, vol. 55, no. 5, pp. 5078-5088, 2019. DOI: 10.1109/TIA.2019.2919497.

[24] A. Azizi, S. Peyghami, H. Mokhtari, and F. Blaabjerg, "Autonomous and decentralized load sharing and energy management approach for DC microgrids," Electric Power Systems Research, vol. 177, article no. 106009, 2019. DOI: 10.1016/j.epsr.2019.106009.

[25] D. Shi, R. Sharma, and Y. Ye, "Adaptive control of distributed generation for microgrid islanding," IEEE PES ISGT Europe, 2013, pp. 1-5. DOI: 10.1109/ISGTEurope.2013.6695471.

[26] S. V. Kulkarni and D. N. Gaonkar, "Improved droop control strategy for parallel connected power electronic converter based distributed generation sources in an Islanded Microgrid," Electric Power Systems Research, vol. 201, article no. 107531, 2021. DOI: 10.1016/j.epsr.2021.107531.

[27] P. Tian and L. Zhang, "Big data mining based coordinated control discrete algorithm of independent micro grid with PV and energy," Microprocessors and Microsystems, vol. 82, article no. 103808, 2021. DOI: 10.1016/j.micpro.2020.103808.

[28] A. Khaligh and C. Omer, "Chapter 1- Solar Energy Harvesting," In: Energy Harvesting, 2nd Edition, CRC Press, pp. 1- 116, Boca Raton, 2010. DOI: 10.1201/9781439815090.

[29] S. Modi, K. Kevin, and P. Usha, "Mathematical modeling, simulation and performance analysis of solar cell," 2018 International Conference on Power Energy, Environment and Intelligent Control (PEEIC), pp. 730-734, 2018. DOI: 10.1109/PEEIC.2018.8665568.

[30] S. Wang, J. Qiu, L. Zhu, T. Ding, and A. –M. Luai A-M, IOP Conference Series: Earth & Environmental Science, vol. 199, no. 5, pp. 1-9, 2018. DOI:10.1088/1755-1315/199/5/052049.

[31] S. M. Mousavi and G. M. Nikdel, "Various battery models for various simulation studies and applications," Renewable and sustainable energy reviews, vol. 32, pp. 477-485, 2014. DOI: 10.1016/j.rser.2014.01.048.

[32] O. Tremblay and L. -A Dessaint L-A, "Experimental validation of a battery dynamic model for EV applications," World Electric Vehicle Journal, vol. 3, no. 2, pp. 289-298, 2009. DOI: 10.3390/wevj3020289.